Supplementary data

Table S1. Calculated lattice constants a and c (in units of Å), lattice constants ratio c/a, the *A*-*B* layer spacing $d_{A\text{-}B}$, *A*-*C* layer spacing $d_{A\text{-}C}$, and *B*-*C* layer spacing $d_{B\text{-}C}$, along the polar axis (in units of Å), ratio of electronegativity difference $\Delta\chi = (\chi_B - \chi_A)/(\chi_C - \chi_A)$, band gap E_g (in units of eV), elastic constant C_{ij}, (in units of GPa), and spontaneous electric polarization P_S (in units of C/m^2) of the hexagonal $A^{I}B^{IV}C^{V}$ semiconductors. The available experimental lattice parameters (NaSnN,[1] NaSnP,[2] NaSnAs,[2] KSnAs,[3] and KSnSb[3]) are also included (in parentheses).

	a	c	c/a	$d_{A\text{-}B}$	$d_{A\text{-}C}$	$d_{B\text{-}C}$	$\Delta\chi$	E_g	C_{11}	C_{12}	C_{13}	C_{33}	C_{44}	P_S
LiGeN	2.98	9.32	3.13	2.37	1.30	0.98	0.45	1.46	252	50	13	115	19	1.82
LiGeP	3.56	10.01	2.81	2.02	1.78	1.21	0.63	0.21	123	24	23	48	20	1.42
NaGeN	3.07	10.41	3.39	2.57	1.71	0.93	0.45	1.70	208	44	18	131	26	1.85
NaGeP	3.62	11.32	3.13	2.36	2.12	1.18	0.63	0.54	109	23	18	61	18	1.38
NaGeAs	3.76	11.41	3.03	2.28	2.18	1.24	0.64	0.25	92	21	18	51	16	1.30
NaGeSb	4.02	11.80	2.94	2.13	2.40	1.37	0.71	0.02	72	18	15	39	12	1.18
KGeN	3.16	11.54	3.65	2.88	1.97	0.91	0.48	1.64	150	41	20	132	32	1.70
KGeP	3.73	12.28	3.29	2.65	2.35	1.14	0.66	0.77	84	25	19	64	23	1.28
KGeAs	3.87	12.36	3.19	2.57	2.40	1.20	0.67	0.42	70	21	18	55	20	1.20
KGeSb	4.12	12.82	3.11	2.45	2.64	1.32	0.73	0.35	59	18	15	43	15	1.10
LiSnN	3.24	9.90	3.05	2.65	1.13	1.17	0.37	1.03	181	49	12	67	7	1.38
NaSnN	3.33 (3.33)	10.89 (10.89)	3.27	2.79	1.58	1.08	0.38	1.05	158	38	15	88	15	1.47
NaSnP	3.87 (3.88)	11.64 (11.66)	3.00	2.58	1.92	1.32	0.52	0.56	81	20	16	44	13	1.13
NaSnAs	4.01 (4.00)	11.66 (11.73)	2.91	2.49	1.97	1.38	0.53	0.22	68	17	17	37	13	1.08
KSnN	3.41	12.03	3.53	3.09	1.87	1.05	0.41	1.19	123	34	16	92	21	1.39
KSnP	3.97	12.66	3.18	2.85	2.20	1.28	0.56	0.89	67	21	16	47	17	1.08
KSnAs	4.11 (4.10)	12.70 (12.84)	3.09	2.77	2.25	1.33	0.56	0.44	58	18	16	40	16	1.02
KSnSb	4.37 (4.36)	12.99 (13.15)	2.97	2.62	2.45	1.43	0.62	0.37	47	16	14	32	14	0.94

Table S2. The Born effective charge [$Z^*_{33}(A)$, $Z^*_{33}(B)$, and $Z^*_{33}(C)$], internal atomic relaxations in response to the longitudinal strain $\{\partial u[(B)-(A)]/\partial\varepsilon_c$ and $\partial u[(C)-(A)]/\partial\varepsilon_c\}$, clamped-ion ($e^0_{3i}$), internal-strain ($e^i_{3i}$), and total ($e_{3i}$) longitudinal and transverse piezoelectric stress coefficients (in units of C/m^2), and longitudinal (d_{33}) and transverse (d_{31}) piezoelectric strain coefficients (in units of pC/N), of the hexagonal $A^{\mathrm{I}}B^{\mathrm{IV}}C^{\mathrm{V}}$ semiconductors. Materials with negative longitudinal piezoelectric effect are underscored.

	$Z^*_{33}(A)$	$Z^*_{33}(B)$	$Z^*_{33}(C)$	$\frac{\partial u[(B)-(A)]}{\partial\varepsilon_c}$	$\frac{\partial u[(C)-(A)]}{\partial\varepsilon_c}$	e^0_{33}	e^i_{33}	e_{33}	e^0_{31}	e^i_{31}	e_{31}	e_{15}	d_{33}	d_{31}	d_{15}
<u>LiGeN</u>	1.63	0.53	−2.16	0.13	0.05	−0.36	−0.19	−0.55	−0.23	0.05	−0.18	−0.66	−4.70	−0.38	−35.37
LiGeP	1.92	−0.35	−1.57	0.09	−0.03	0.02	0.03	0.05	−0.30	−0.10	−0.40	0.16	4.20	−3.36	8.02
<u>NaGeN</u>	1.44	0.47	−1.91	0.09	0.02	−0.20	0.01	−0.19	−0.22	0.04	−0.18	−0.41	−1.24	−0.64	−15.71
NaGeP	1.72	−0.30	−1.42	0.07	−0.02	−0.01	0.03	0.01	−0.18	−0.06	−0.24	−0.10	1.42	−2.02	−5.74
NaGeAs	1.79	−0.52	−1.26	0.05	−0.05	0.03	0.08	0.12	−0.23	−0.04	−0.26	0.01	4.38	−3.03	0.53
NaGeSb	1.86	−0.78	−1.08	0.03	−0.08	0.10	0.15	0.25	−0.23	−0.03	−0.26	0.15	10.05	−4.56	12.24
<u>KGeN</u>	1.61	0.33	−1.94	0.11	0.06	−0.07	−0.31	−0.38	−0.18	−0.03	−0.21	−0.40	−2.67	−0.81	−12.58
<u>KGeP</u>	1.71	−0.37	−1.34	0.07	0.00	0.01	−0.07	−0.06	−0.15	−0.06	−0.21	−0.13	0.21	−1.97	−5.94
KGeAs	1.75	−0.71	−1.04	0.05	−0.02	0.07	−0.02	0.05	−0.24	−0.07	−0.31	−0.08	3.75	−4.18	−4.20
KGeSb	1.79	−0.92	−0.88	0.01	−0.07	0.11	0.10	0.21	−0.23	−0.08	−0.30	0.04	8.68	−5.60	2.79
<u>LiSnN</u>	1.67	0.48	−2.15	0.17	0.08	−0.33	−0.31	−0.64	−0.17	0.17	−0.01	−0.60	−9.61	0.46	−82.35
<u>NaSnN</u>	1.52	0.35	−1.87	0.11	0.04	−0.21	−0.09	−0.30	−0.19	0.09	−0.10	−0.36	−3.36	−0.27	−24.20
<u>NaSnP</u>	1.76	−0.14	−1.63	0.10	0.00	−0.07	−0.05	−0.12	−0.21	−0.06	−0.27	−0.19	−0.84	−2.49	−15.07
<u>NaSnAs</u>	1.83	−0.39	−1.44	0.08	−0.02	0.00	−0.03	−0.02	−0.26	−0.05	−0.32	−0.13	3.34	−4.40	−10.15
<u>KSnN</u>	1.53	0.32	−1.85	0.12	0.07	−0.11	−0.26	−0.37	−0.12	0.04	−0.09	−0.36	−3.97	−0.16	−17.31
<u>KSnP</u>	1.66	−0.18	−1.48	0.10	0.03	−0.04	−0.13	−0.17	−0.14	−0.04	−0.19	−0.21	−2.53	−1.69	−12.63
<u>KSnAs</u>	1.70	−0.47	−1.23	0.08	0.01	0.02	−0.10	−0.09	−0.20	−0.05	−0.26	−0.17	0.58	−3.49	−10.94
KSnSb	1.77	−0.69	−1.08	0.05	−0.03	0.07	0.00	0.07	−0.21	−0.06	−0.26	−0.05	7.41	−5.88	−4.02

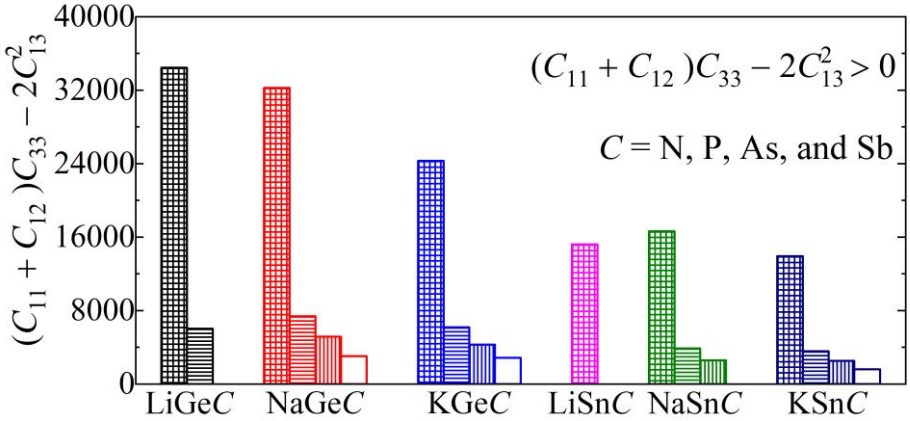

Fig. S1. Born criterion for mechanical stability $(C_{11}+C_{12})C_{33}-2C_{13}^2$ for the hexagonal $A^{I}B^{IV}C^{V}$ semiconductors. Other criteria ($C_{44}>0$ and $C_{11}-|C_{12}|>0$) can be found in Table S1.

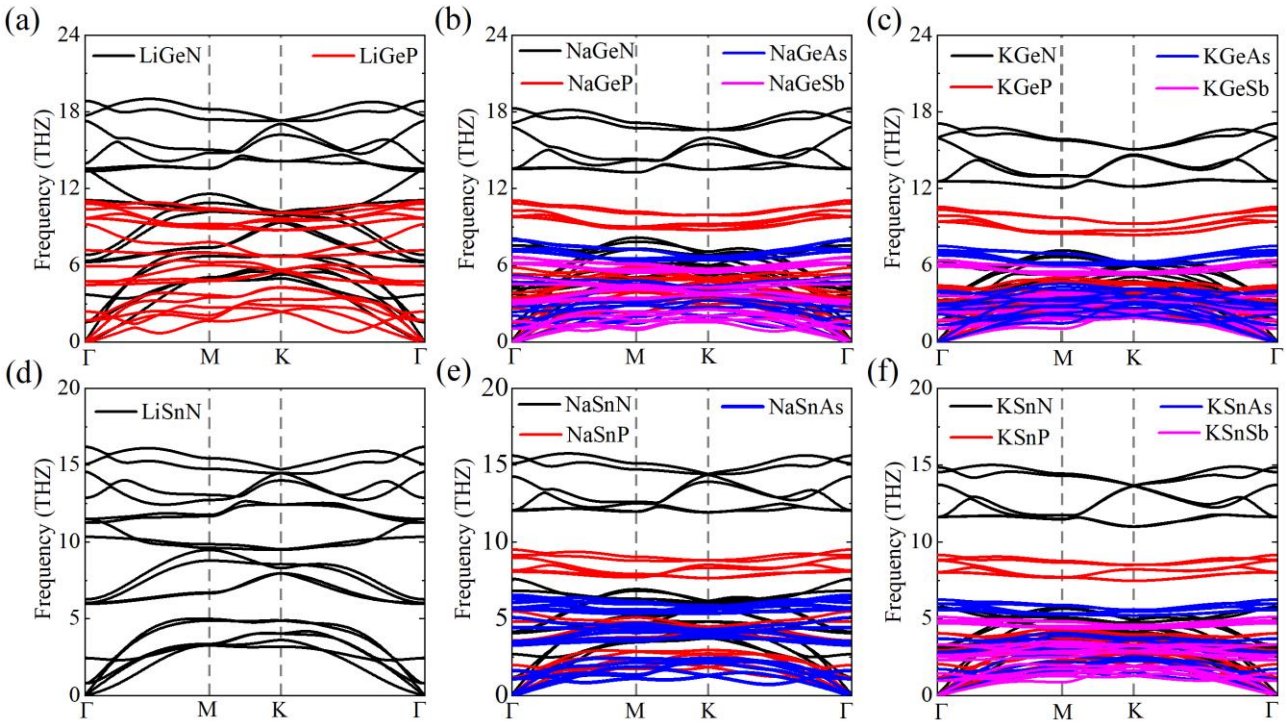

Fig. S2. Phonon dispersion relations for the hexagonal $A^{I}B^{IV}C^{V}$ semiconductors.

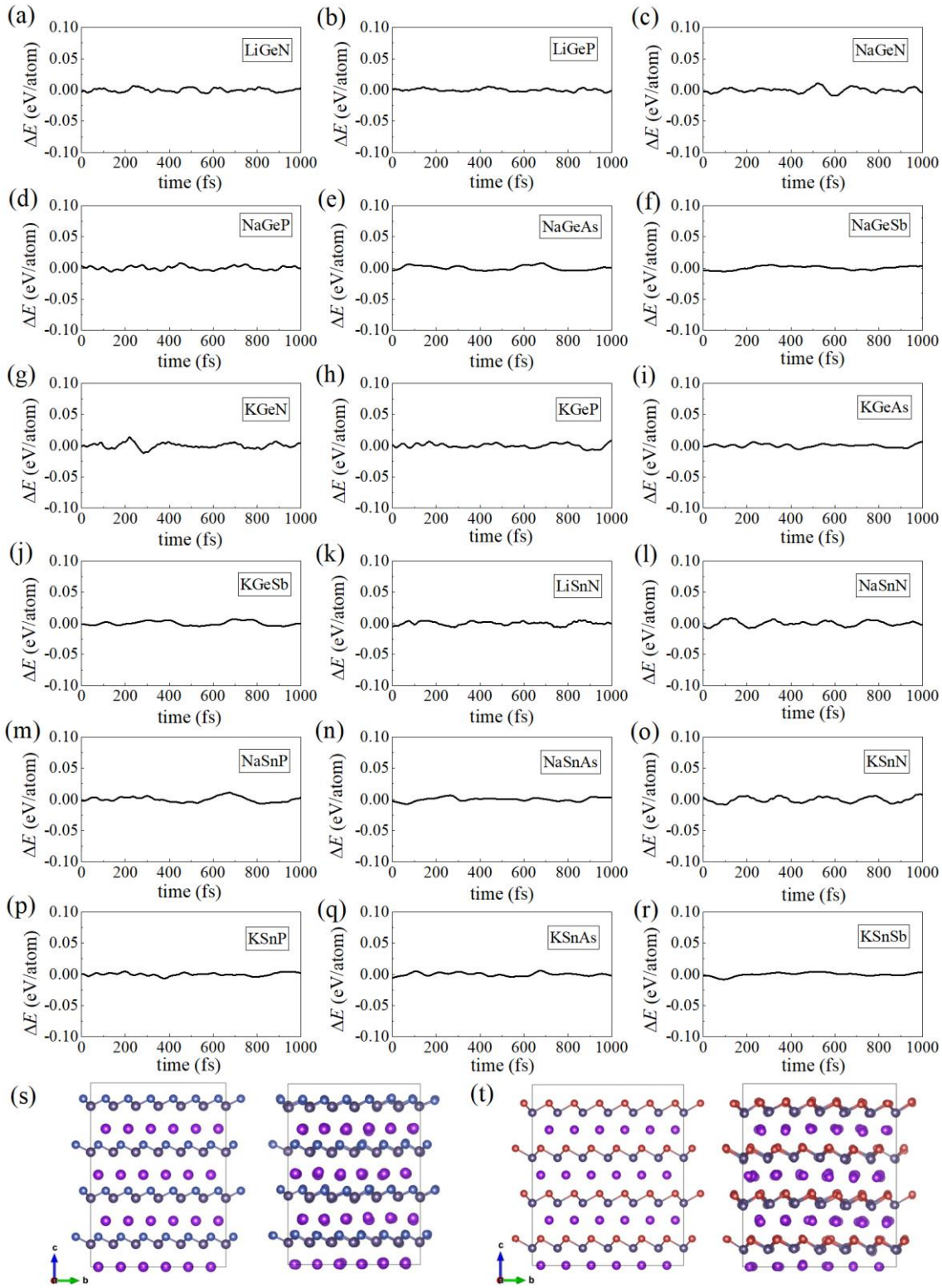

Fig. S3. (a-r) The evolution of the total energy during the *ab initio* molecular dynamics (AIMD) simulations at 300 K for the hexagonal $A^{I}B^{IV}C^{V}$ semiconductors. AIMD simulations are performed on a 6 × 6 × 2 supercell. Instantaneous structure at the initial and final AIMD steps for (s) KGeN and (t) KGeSb.

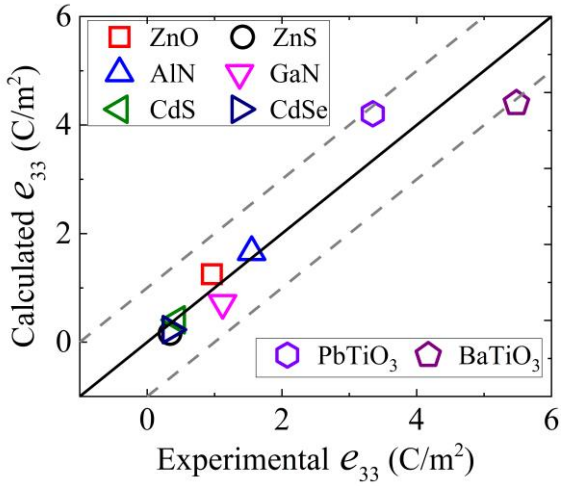

Fig. S4. Calculated longitudinal piezoelectric stress coefficients e_{33} vs experimentally measured e_{33} for wurtzite semiconductors (e.g., ZnO,[4] ZnS,[5] AlN,[6] GaN,[6] CdS,[7] and CdSe[7]) and ferroelectric perovskites (e.g., $PbTiO_3$[8] and $BaTiO_3$[9]).

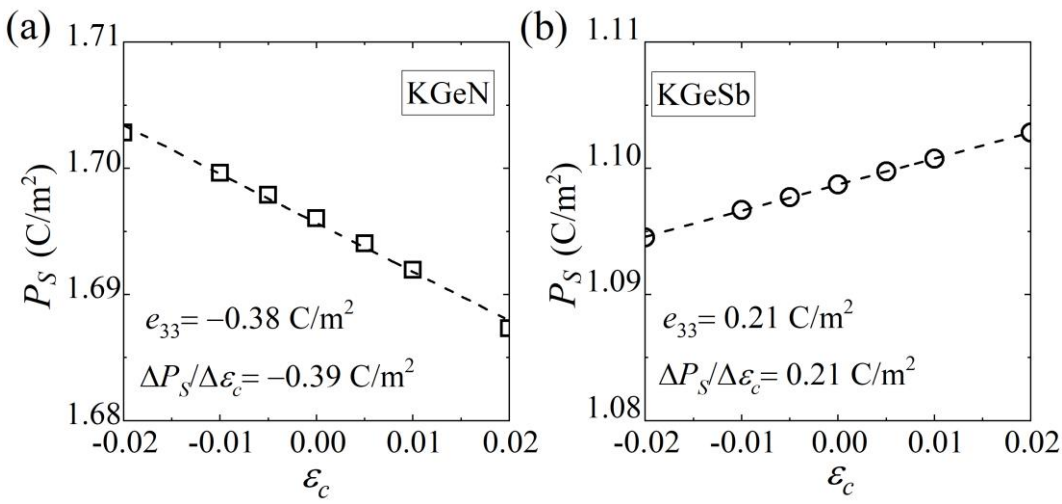

Fig. S5. Spontaneous polarization P_S for (a) KGeN and (b) KGeSb as a function of longitudinal strain ε_c (the slope corresponds to piezoelectric stress coefficient e_{33}).

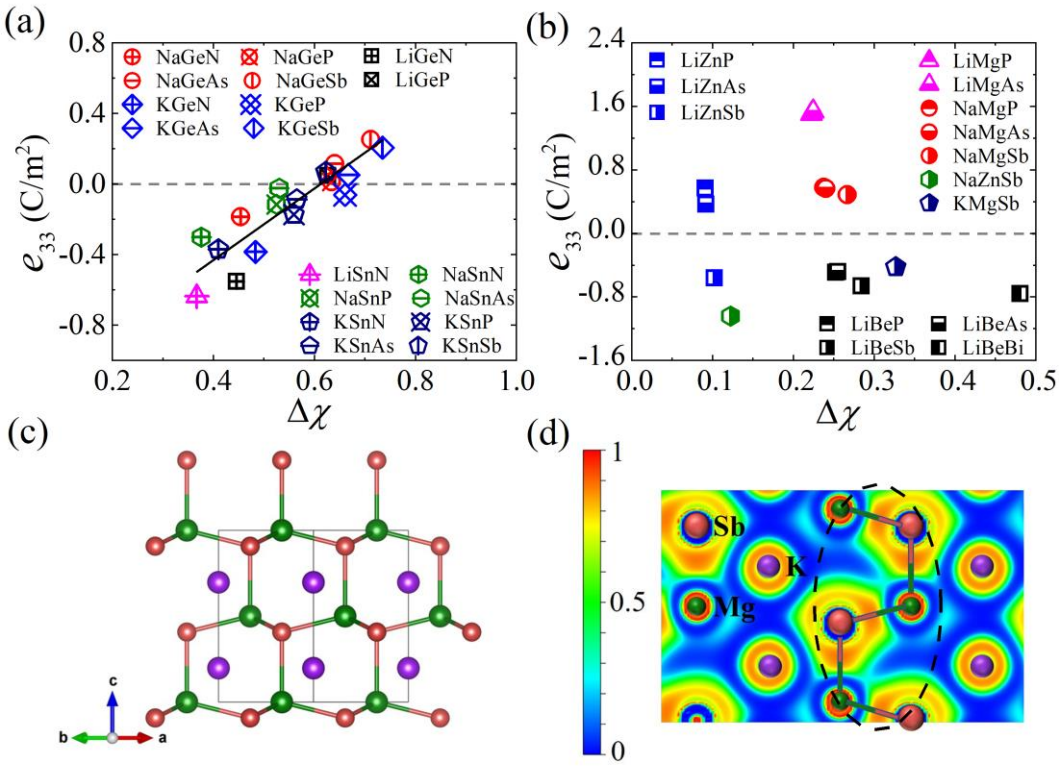

Fig. S6. The longitudinal piezoelectric stress coefficients e_{33} versus the ratio of electronegativity difference $\Delta\chi = (\chi_B - \chi_A)/(\chi_C - \chi_A)$ for the hexagonal (a) $A^{I}B^{IV}C^{V}$ and (b) $A^{I}B^{II}C^{V}$ semiconductor. The e_{33} values for hexagonal $A^{I}B^{II}C^{V}$ semiconductor are from Ref. 10. (c) Crystal structures of the hexagonal $A^{I}B^{II}C^{V}$ semiconductor and (d) the electron localization function (ELF) projected along the [110] plane for KMgSb.

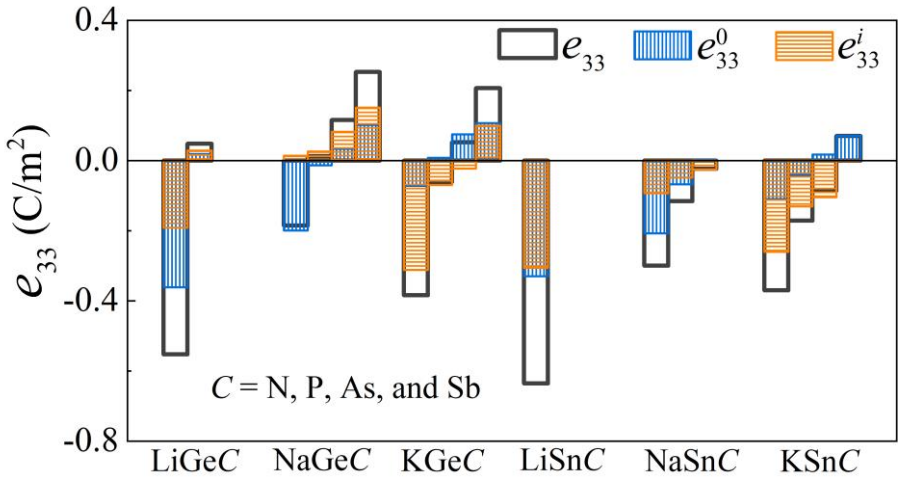

Fig. S7. The calculated clamped-ion (e_{33}^{0}), internal-strain (e_{33}^{i}), and total (e_{33}) piezoelectric coefficients of the hexagonal $A^{I}B^{IV}C^{V}$ semiconductors.

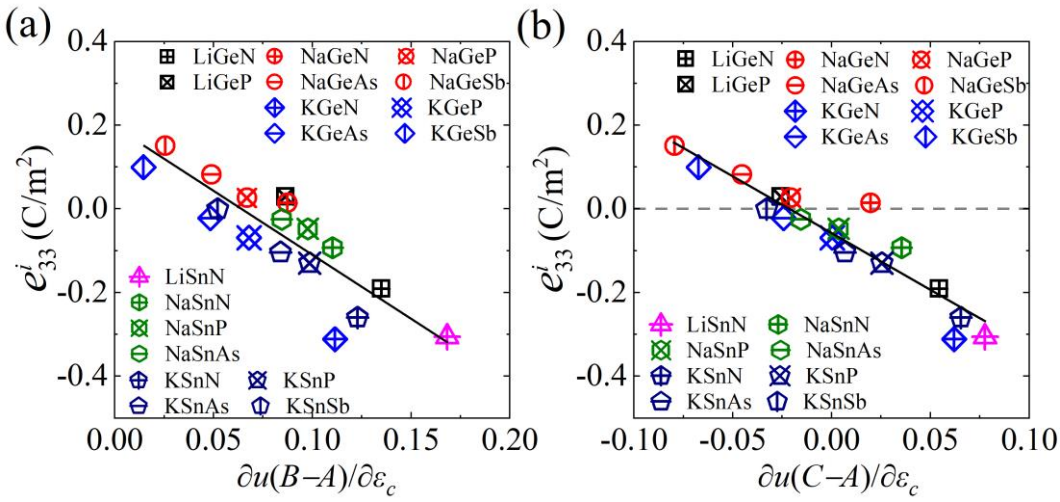

Fig. S8. Calculated internal-strain longitudinal piezoelectric stress coefficients e^i_{33} vs internal atomic relaxations in response to the longitudinal strain $\{\partial u[(B)-(A)]/\partial\varepsilon_c,\ \partial u[(C)-(A)]/\partial\varepsilon_c\}$ for the hexagonal $A^{\mathrm{I}}B^{\mathrm{IV}}C^{\mathrm{V}}$ semiconductor.

References

1. N. S. P. Watney, Z. A. Gál, M. D. S. Webster and S. J. Clarke, *Chem. Commun.*, 2005, 4190-4192.
2. Z. Lin, G. Wang, C. Le, H. Zhao, N. Liu, J. Hu, L. Guo and X. Chen, *Phys. Rev. B*, 2017, **95**, 165201.
3. K. H. Lii and R. C. Haushalter, *J. Solid State Chem.*, 1987, **67**, 374-378.
4. I. B. Kobiakov, *Solid State Commun.*, 1980, **35**, 305-310.
5. J. G. Gualtieri, J. A. Kosinski and A. Ballato, *IEEE Trans. Ultrason. Ferroelectr. Freq. Control*, 1994, **41**, 53-59.
6. I. L. Guy, S. Muensit and E. M. Goldys, *Appl. Phys. Lett.*, 1999, **75**, 4133-4135.
7. D. Berlincourt, H. Jaffe and L. R. Shiozawa, *Phys. Rev.*, 1963, **129**, 1009-1017.
8. Z. Li, M. Grimsditch, X. Xu and S. K. Chan, *Ferroelectrics*, 1993, **141**, 313-325.
9. Z. Li, S. K. Chan, M. H. Grimsditch and E. S. Zouboulis, *J. Appl. Phys.*, 1991, **70**, 7327-7332.
10. S. Liu and R. E. Cohen, *Phys. Rev. Lett.*, 2017, **119**, 207601.